Proceedings of the ASME 2021
International Mechanical Engineering Congress and Exposition
IMECE2021
November 1-5, 2021, Virtual, Online

IMECE2021-69775

SHOCK WAVE HEATING:
A NOVEL METHOD FOR LOW-COST HYDROGEN PRODUCTION

Pejman Akbari
California State Polytechnic University
Pomona, California
pejmanakbari@cpp.edu

Colin D. Copeland
Simon Fraser University
Vancouver, Canada
colin_copeland@sfu.ca

Stefan Tüchler
University of Bath
Bath, United Kingdom
stefan.tuechler@bath.edu

Mark Davidson
New Wave Hydrogen, Inc.
Gainesville, Florida
mark@thetechtoybox.org

Seyyed V. Mahmoodi-Jezeh
Simon Fraser University
Vancouver, Canada
vahid_mahmoodi@sfu.ca

ABSTRACT

This study introduces a new method of methane pyrolysis in a rotary chemical reactor using wave rotor technology. The patented technology has been developed by New Wave Hydrogen, Inc. (New Wave H_2 or NWH_2). The concept introduces an efficient method of hydrogen production driven by shock wave gasdyanmics, with no direct CO_2 emissions and no water use. The New Wave Reformer is based on wave rotor designs where unsteady shock waves are generated within channels arrayed around a rotating drum. As in a typical wave rotor wave cycle, a sharp pressure increase occurs behind a reflected shock wave, resulting in a proportional increase in gas temperature. This temperature amplification can be used to initiate a thermal decomposition reaction in gaseous constituents. Past studies have proven that a wave reformer with onboard reactions can reform heavy hydrocarbon gases into lighter hydrocarbon products. The current NWH_2 study explores how a wave rotor can employ pressurized natural gas as a driver gas for compression heating of a low-pressure hydrocarbon fuel inside the channels of a wave reformer, resulting in the decomposition of methane into hydrogen and carbon black. This study first reviews past efforts ranging from conceptual patents to experimental studies utilizing different wave cycles for rapid heating of gases in gas-phase chemical reactions. Examples of such reactions include the formation of acetylene from methane and the formation of nitric oxide from air. In ongoing research, the authors introduce a wave cycle that uses a dual-stage gas compression process designed to prolong reaction time within the channels, addressing a key factor in high methane-to-hydrogen conversion. The process has been modeled numerically using a customized version of the Tüchler-Copeland experimentally-validated quasi-one-dimensional CFD code. The computational results provide data used in the prediction of flow fields inside the channels and at the inflow/outflow ports of the reactor.

Keywords: wave reformer, wave rotor, methane pyrolysis, shock heating, wave chemical reactor, hydrogen.

1. INTRODUCTION

The combustion of fossil fuels is considered a prime contribution to global climate change. Hydrogen, as a carbon-free energy carrier, may play a critical role in reducing global greenhouse gas (GHG) emissions. Hydrogen can be used in a broad range of existing and potential applications including electrical generation, transportation, propulsion, and heating. One of the major barriers to widespread hydrogen adoption, however, is the cost and environment impact of its production. Currently, hydrogen produced from electrolysis powered by renewable energy sources (e.g. solar or wind power) is considered “green hydrogen” [1]. More commonly, hydrogen is produced from fossil fuels such as through the reforming of natural gas [2]. In particular, steam methane reforming (SMR) is a well-developed method for hydrogen production in industry. In this approach, methane and steam are heated until they react to

yield hydrogen and CO_2. Therefore, this method not only continuously produces greenhouse gases in large quantities, but it also requires a large input of thermal energy which is typically derived from hydrocarbon fuels, further contributing to emission problems. Additionally, the process has a water demand in production of steam which limits this technology in places that face water limitations and adds a potential water supply impact.

Considering drawbacks of SMR, the direct decomposition of methane from natural gas provides a more environmentally friendly and efficient process. In this process, referred to as methane pyrolysis or methane cracking, methane is heated to temperatures sufficient to break the carbon-hydrogen bonds and decomposing methane into its elements: hydrogen and solid carbon ($CH_4 \rightarrow C + 2\ H_2$). The governing reaction is endothermic and requires an energy input, typically from conventional or renewable electrical energy. In methane pyrolysis, the absence of oxygen in the reaction eliminates CO_2 and CO by-products. No water is consumed, and the produced carbon may have qualities that can be marketed and used in a variety of traditional and novel applications, or it can be securely stored for future use. Different methods of methane decomposition processes have been developed including direct thermal cracking at very high temperatures, catalyzed thermal decarbonization, and plasma-torch driven methane pyrolysis [3]. A limited number of these techniques have been commercialized. These conversion processes differ in relation to the reactor type, the use of a catalyst, and the source of process-related energy.

To efficiently achieve high temperatures required for direct thermal methane decomposition, New Wave Hydrogen (NWH_2) has designed and is demonstrating a wave reformer utilizing shock heating. In comparison with SMR, NWH_2 offers a high-temperature thermal reforming process that uses no water and produces no direct CO_2 emissions. The core component is an existing proven technology (a wave rotor) combined with a well-known process (methane pyrolysis), to produce hydrogen in a low-cost, efficient reactor. The invention overcomes some of disadvantages of the existing techniques by employing unsteady shock waves that can produce high temperatures very rapidly with lower energy consumption per unit mass of product. As described further in this paper, a unique attribute of the NWH_2 process is the use of shock wave gas temperature amplification, rather than electricity driven heating. The wave reformer benefits from the use of the pressure already embodied in a pipeline or feedstock line and the energy transfer by the shock wave. This is an interesting distinction relative to competing methods of methane pyrolysis. Thus, the impact of this technology is significant because the production of hydrogen from methane within a wave rotor reformer can utilize existing natural gas supply infrastructure with little change to energy or water supplies.

Wave rotors are unique in many ways. A few of which include the ease in scaling and the potential for the inflowing gas to maintain a wall-material temperature lower than the peak temperature in the inner channel. Conventional turbomachines exchange fluid energy by shaft work. In a wave rotor, the energy exchange between two fluids is conducted by the unsteady wave dynamics and there is no shaft power exchanged with the flow. This is, in part, why the footprint remains small even with large flows and supports the ease in scaling. This ease in scaling allows the wave reformer to support both small, distributed hydrogen production and large-scale centralized production. Using natural gas as the feedstock allows the use of existing infrastructure (e.g., existing and planned natural gas pipeline distribution systems). It is possible that the system could be installed at gas let-down stations, adding value to the pressure loss at these junctures by producing hydrogen.

Using the existing natural gas infrastructure may be an important distinction, particularly when combined with a process that produces no direct CO_2 emissions and has a low electricity demand. Currently, SMR as a predominant method of hydrogen production releases a high multiple of tonnes CO_2 (~10x) and uses many kiloliters of water (~15 kliters) per tonne of hydrogen produced [4]. SMR combined with carbon capture and storage (CCS) is termed ‘blue hydrogen’. In areas where CO_2 pipelines and CCS are not already in place, SMR with CCS may have long timelines and risks associated with infrastructure financing and build-out. Proton Exchange Membrane (PEM) electrolysis challenges are reported to include high electricity demand, water use, and total cost [5]. Electrolysis using conventional power sources is not green hydrogen. With fossil-based electrical power, the high electricity demand of electrolysis has a relatively high CO_2 emission impact. Thus, currently, wide adoption of electrolysis will require a rapid, co-build out of the renewable power base to make any near-term impact. The potential global costs of building a new renewable power infrastructure base, to support a high-electricity demand hydrogen production process, may be challenging.

The NWH_2 process appears to embody the benefits of each current technology, i.e., no direct emissions and a low electricity demand, potentially without a dependence on extensive infrastructure investments. This could remove hurdles in a region’s transition to hydrogen fuels, possibly accelerating a path to significant GHG emission reductions.

This paper first describes wave rotors, their working principles, and a range of applications that have used wave rotors over the past several decades. Then, particular attention is given to hydrocarbon pyrolysis in wave rotors where there is a scarcity of published work. That said, general shock wave research of hydrocarbon pyrolysis is not unusual. There are a number of studies using either a supersonic normal shock reactor [6, 7] or a traditional shock tube [8, 9], or a combination of both [10]. The

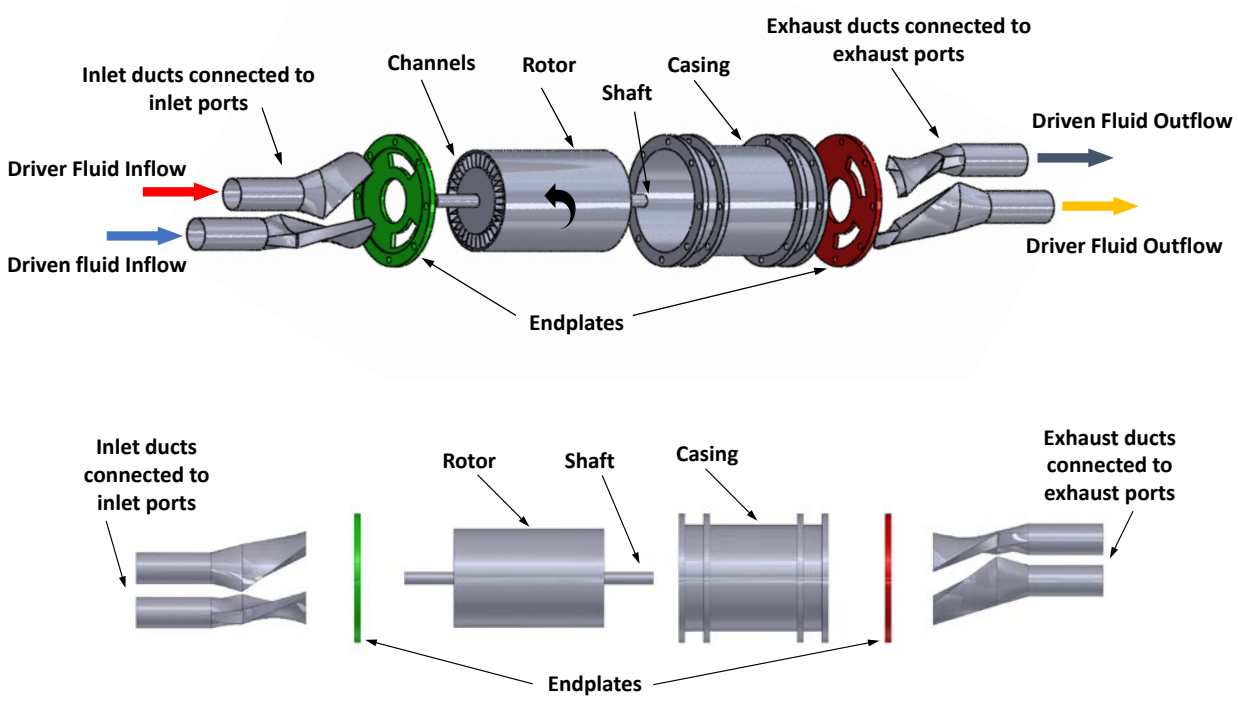

Figure 1: Schematic configuration of a four-port wave rotor.

latter three references [8-10] specifically studied methane pyrolysis and demonstrated the importance of both temperature and reaction time. Unlike prior studies, the NWH_2 process involves no combustion; the heating is purely shock wave driven. Moving forward, several wave cycles will be discussed that were proposed in past investigations employing shock compression and its associated temperature rise to achieve direct pyrolysis of hydrocarbons onboard a rotor. In many past wave rotor applications, the pressure source for shock heating onboard the rotor was combustion driven, but in the wave reformer introduced here the energy input is largely provided from the energy contained in the pressurized natural gas pipeline. This paper also introduces a new wave cycle that adds incremental benefits over previous wave cycles in terms of peak temperature and reaction residence time.

2. WAVE ROTOR DESCRIPTION

The wave rotor is a direct energy exchange device that utilizes one-dimensional pressure wave action for the transfer of mechanical energy between two compressible fluid flows which are at different pressure levels. There are a multitude of wave rotor designs covering a range of applications [11]. A typical wave rotor consists of a cylindrical rotor with an array of long axial channels arranged uniformly around its periphery. The rotor spins between two stationary endplates through which the flow enters and exists. The endplates house a set of ports to accommodate the incoming and outgoing fluids. For instance, Fig. 1 shows a schematic of a four-port wave rotor which uses two inlet ports and two outlet ports. Gaps between the rotor and the endplates (green and red colors) are exaggerated for clarity. In practice the gap is kept very small to minimize gas leakage. Alternatively, the endplates may use sealing material at the rotor-endplate contact. The rotor spins through a drive shaft that may be gear-driven, belt-driven, or direct-driven by an electrical motor (not shown in Fig. 1). The power required to maintain typical rotational speeds is generally quite low. The only shaft power needed is that required to overcome rotor windage and the friction in the bearing and contact sealing, if used. Alternatively, rotors can be designed to be self-driving (i.e. a free-running rotor) using the flow angles and the momentum of the inflow or outflow gases [12]. In this case, the driving force to turn the rotor comes from the fluid flows. If the channels are not straight (e.g. curved channels), net power can be extracted from the rotor (similar to a turbine), in addition to the work exchange between the fluid streams [13].

Each channel arrayed around the rotor operates independently, similar to an array of individual shock tubes. The entry and exit ports function as rotating valves, resembling the diaphragm in a conventional form of shock tube. The rapid opening and closing of the rotating channel forms a series of unsteady compression and expansion waves when the channel ends periodically rotate past the inlet/exit ports and regions of closed endplates. To generate compression waves, the channels are exposed to a high-pressure port of a driver gas source. The driver gas compresses the driven gas within the channels. The compression energy exchange is analogous to a mechanical

piston. To generate expansion waves, the channels are exposed to an open port in the exit endplate, whereby the gases and any reactant products in the channels expand and discharge. The timing of the port openings and closings drive the unsteady waves acting onboard the rotor. These unsteady waves are deliberately created and are employed to direct gas into and out of the rotor channels. When there is a sequence of identical independent channels arrayed around the rotating central rotor, the result is a nearly continuous flow in and out of the ports. Rotational motion of the drum gives precise control of the wave processes. The process is repeated in each revolution, producing a periodic wave pattern, or "wave cycle".

In Fig. 1, the low-pressure driven gas enters the rotor from an inlet port at one end of the rotor when the channels are aligned with the port. As the rotor rotates, the rotor channels filled with the driven gas are exposed to the high-pressure driver gas inlet port when they are aligned with that port. Due to the pressure difference between the driver and driven gases, the driver gas is forced into the channels. This initiates shock waves that pass through the channels and compress the driven fluid already in the channels. The driver gas pressure, in part, determines the shock strengths generated within the device. Continuous rotation of the drum moves the channels between the closed endplates that bring the channel flow to rest. The energized driven fluid leaves the channels through the corresponding outlet port at the opposite end assisted by expansion waves generated at the channel ends. By further rotation, the de-energized driver gas is also scavenged out of the drum through the corresponding outlet port and the cycle repeats itself. By carefully selecting port locations and their widths, an efficient transfer of energy can be obtained between flows in the connected ducts with minor mixing effects at the gas interfaces. The net effect is an increase in stagnation pressure and temperature of the compressing gas and a decrease in stagnation pressure and temperature for the expanding gas, similar to a mechanically coupled gas compressor and turbine. Here, gasdynamic waves replace the mechanical blades in a turbo device. The gasdynamic process achieves the energy exchange between the fluids.

A single channel in a wave rotor is comparable to a classic shock tube. Both control the transfer of energy between driver and driven gases by means of unsteady waves. In fact, the wave rotor can be visualized as a rotating multi-shock tube device. However, a rotor with high rotating speed establishes periodic unsteady flow processes within the rotating passages and nearly steady flow in the inlet/outlet ports. Additionally, instead of a single event initiated by a diaphragm rupture, the wave rotor benefits from pre-selected sliding valve timing (e.g. port opening/closing) that allows the designer to create a wide variety of shock interactions within the channel for a plurality of purposes in a nearly continuous process. In other words, the wave rotor can be considered as the continuous-flow analogue of the single-pulse shock tube and various wave cycles can be designed for different applications. Thus, wave rotors support the study of high-temperature phenomena in gases over longer operational times.

2.1 Inner Working Principles

A wave diagram is introduced in this section to aid in the description of the physical phenomena occurring in the channels. Wave diagrams are helpful for visualizing the unsteady flow processes taking place in the channels. The wave diagram portrays the annular arrangement of the inlet and outlet ports, solid walls reflecting the endplates, the wave fronts, and gas interfaces during each phase of the cycle. In design stages, this can aid in the generation of new cycles and supports rapid comparative evaluation between cycle designs.

A wave diagram is constructed by conceptually unwrapping the rotor channels in an x-t (distance- time) or x-θ (distance-circumferential angle) domain. It displays a time-history of the flow in any single wave rotor passage as it moves through the wave rotor cycle. Since the same processes occur in each of the rotor channels, the operation can best be understood by explaining what happens in one of the rotor channels during one complete revolution of the drum. Wave diagrams can also be viewed as an instantaneous snapshot of the flow in the entire rotor with the rotational motion of the rotor channels represented by straight translatory motion (i.e. unwrapped view of the rotor). Figure 2 schematically illustrates an unwrapped demonstration of a single channel in a through-flow wave rotor as an example. The channel is shown moving upward or vertically in the figure in a single cycle of the wave rotor. It should be understood that the top of each wave diagram is looped around and joined to the bottom of the diagram, i.e. each wave cycle is repetitive. The vertical solid lines on each side of the channels represent the stationary endplate locations around the circumference when the inlet and outlet ports are closed. The diagonal lines are the propagation lines (trajectories) of the waves and contact surfaces

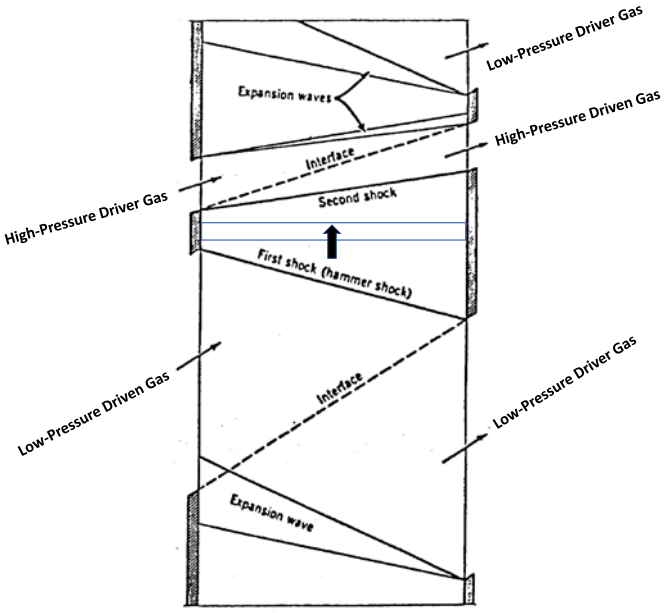

Figure 2: Wave diagram of a four-port wave rotor.

(interfaces between the fluids). Wave interactions at interfaces are often ignored. In this four-port design, each cycle consists of two inflow ports where the fresh driver and driven fluids ingress into the rotating channel, and two outflow ports where the energized-driven gas and de-energized driver gas are discharged from the rotor channel. The following section describes the events occurring in a channel during one complete cycle and how shock and expansion waves are effectively employed to transfer energy between the gases.

The generic cycle shown in Fig. 2 can be separated into high-pressure and low-pressure processes. In the high-pressure process, the low-pressure driven gas is energized by the high-pressure driver gas. The low-pressure process is designed to discharge the expanded driver gas from the rotor and to fill and cool the channel with a through-flow of incoming driven gas.

In Fig. 2, the low-pressure part of the cycle begins at the bottom of the diagram where the flow within the channel is entirely filled with the spent driver gas from the prior cycle, and the channel ends are closed. As the right end of the channel opens to the relatively low-pressure outlet port, an expansion fan originates from the leading edge of the outlet port and propagates into the channel, expanding and discharging the driver gas out of the channel. When the expansion fan arrives to the left channel end, the inlet port starts to open and fresh driven gas penetrates the channel from the left. This driven gas is separated by a contact surface (dashed line) from the expanded driver gas leaving the channel from right, i.e. an overlap process. Complete evacuation of the driver gas from the channel is aided by the fresh charge of the driven gas. The closing of the exit port is timed with the arrival of the contact surface to the right end of the channel when the complete scavenge of the driver gas through the exit port is finished. The closing of the exit port generates a weak shock wave (i.e. hammer shock) propagating upstream, stopping the channel gas and increasing its pressure and temperature. When the compression wave meets the upper corner of the inlet port, the port closes leaving the channel fully filled with pre-compressed driven gas.

The high-pressure part of the cycle begins when the fresh driver gas entry port (left side of diagram) suddenly opens. When it opens, the high-pressure driver gas enters the channel and another shock wave is generated. This shock wave travels to the right (in the diagram), compressing the driven gas further. The shock wave causes a substantial rise in pressure. Behind the wave is another contact surface separating the incoming driver gas from the compressed driven gas. This contact surface follows the shock wave to the right slower than the shock wave. The shock wave arrives at the right end of the channel when another exit port opens, expelling the compressed driven gas to the outlet port. Therefore, the low-pressure driven gas that entered the rotor from the inlet port in the low-pressure part of the cycle is compressed and leaves at the opposite end of the rotor through its outlet port in the high-pressure part of the cycle.

As the rotor drum rotates, the inlet port closes cutting off the driver gas flow. This generates an expansion wave that follows the shock wave, bringing the channel flow to rest. The closing of the driven outlet port is designed to be timed with the arrival of the expansion wave and the contact surface fronts at the channel right end. This concludes the high-pressure process. At this very moment, the only gas trapped in the channel is the expanded driver gas, and a new cycle begins. Note that the high-pressure driver gas and the low-pressure driven gas enter and leave at opposite ends of the rotor, creating a through-flow pattern internally. The energy gain in the driven gas is made up by a corresponding energy loss in the driver gas. This sequence of events occurs successively in each of the rotor channels as the drum spins, resulting in a continuous supply of energized gas that is discharged out of its outlet port.

In practice, wave locations deviate from these idealized conditions due to wave interactions and reflections. Also, fluid mixing at gas/gas interfaces are not shown in these simplified wave cycles. Interface skewing, boundary layer flow dynamics, and gradual opening/closing of the channel influence flow fields within the wave rotor channels and are not adequately described by one-dimensional illustrations. Accurate numerical modeling can reveal those details. Even so, the simplified wave diagram is close enough to the actual processes and captures the governing behavior.

3. WAVE ROTOR FOR ENERGY AND CHEMICAL PROCESS APPLICATIONS

In the past few decades, a variety of wave rotor configurations were developed for a wide range of applications. Wave rotors have been successfully utilized in power generation, propulsion, automobiles, chemical processes, refrigeration, and other applications [11]. Most of the work in the U.S. originates from the early efforts of the General Electric Company and General Power Corporation, evolving to recent activities conducted collaboratively by NASA Glenn Research Center, Army Research Laboratory, and Rolls Royce North America [14, 15]. The most recent efforts are conducted by the Air Force Research Laboratory focusing on the testing of small-scale pressure wave superchargers [16]. The majority of the U.S. activity has centered on using wave rotors to enhance the performance of stationary power systems or aeropropulsion engines. However, the application of wave rotors is not limited to gas turbine engines. As example, Brown Boveri Company (BBC) in Switzerland, later Asea Brown Boveri (ABB), has a long and successful history of using wave rotors as superchargers in passenger car and heavy diesel engines. ABB's pressure wave supercharger, termed as the Comprex®, has been used commercially in several passenger car engines [17] and can still be found on the market today. The wave rotor has also been used as a superheater in the past at Cornell Aeronautical Laboratory (CAL) [18-20]. The CAL Wave Superheater was built in 1958 and successfully operated for a decade until decommissioning in 1969. It used heated helium as the driver gas to provide a steady stream of high-temperature high-pressure air for a hypersonic wind tunnel test facility. It compressed and heated air to more than 3500 K and up to 120 atm for periods of seconds. The machine was successful and proved the high temperature capability of wave machinery.

The contributions of the Cornell Aero group to the successful demonstration of an unsteady wave machine is not limited to their Wave Superheater. In fact, in the early 1950s, extensive research was developed in the use of unsteady waves to heat a gas to high reaction temperatures to promote the formation of useful products through the pyrolysis of various hydrocarbon fuels [21]. They also conducted a series of investigations into the thermal fixation of nitrogen directly from air by the generation of nitrogen oxide (NO) by the proper heating and subsequent rapid cooling of air in a chemical shock tube [22]. It was found that at very high temperatures, significant concentrations of NO could be achieved by the shock heating of air. Rose [23] reported NO production in concentrations of 5-7% at high temperatures and pressures (approximately 3000 K and 100 atm), sufficient for economic recovery. Their studies led to a successful series of experiments which provided data on the kinetic rates of NO formation and demonstrated conclusively that nitrogen could be fixed by means of a combination of shock waves and expansion waves in controlled temperature pulses [24]. The success of this work encouraged the Cornell Aero laboratory to extend the concept from a single-shot basis in a single-pulse shock tube to a continuous basis in a wave rotor as a method of commercial production of nitrogen fixation. Because the opening and closing of the passage as it traverses the ports closely simulates the diaphragm opening processes of the shock tube, the same inherent operational principles exist between shock tubes and wave rotors. A series of theoretical studies were carried out to verify the concept [25-27] and the preliminary results were promising [24] even though this method was not further pursued due to competition from other emerging nitrogen fixation techniques in the fertilizer industry.

Recently, NWH_2 proposed hydrogen production through compression-induced pyrolysis of methane using the pressure in natural gas pipelines. Historically, the NWH_2 patent [28], authored by Kielb, describes an example of a four-port wave reformer. Considerable progress in design optimization and system integration has resulted in a range of design options, some of which are described in this paper along with some historical predecessors.

Figure 3 illustrates a wave diagram for a four-port through-flow wave reformer. The red color represents the driver gas (pipeline natural gas) and blue color represents the driven gas (methane to be reformed). The cycle consists of the following steps: charging of reactant (driven) gas into the reformer, charging of driving gas into the reformer, removal of reactant products from the reactor, and removal of spent driver gas from the reactor. The last two processes often occur simultaneously. The diagram is similar to that shown in Fig. 2 with the exception that the primary shock wave compressing the reactant gas is deliberately timed to strike the solid endplate at the far-right end of the channel so that it can reflect from the endplate and also stagnate the flow. It is well recognized that the temperature behind a reflected shock wave is approximately double that behind an incident shock wave, therefore, higher temperatures can be attained by shock reflection. The reflected shock wave passes through the reactant gas wherein the temperature has been

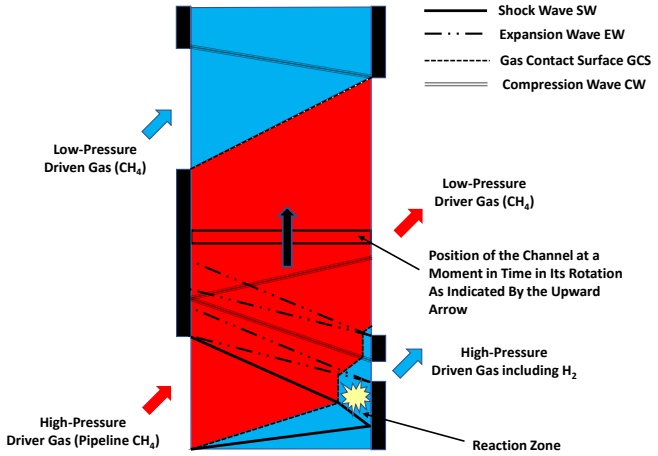

Figure 3: Wave diagram of a through-flow wave reformer.

raised to an intermediate level by the first shock wave, thereby raising the process gas temperature to an even higher level, i.e. maximum temperature. This peak temperature is sufficient to drive methane thermal decomposition. The peak temperature in the reaction zone (yellow, star-shaped area) is a function of the initial temperature of the reactant gas and Mach number of the primary shock wave, which in turn is a function of the pressure ratio between the driver gas and the reactant gas. The required pressure ratio will depend on the reaction temperature that initiates reaction prior to opening the exit port. Meanwhile, the passage of the reflected shock wave brings the reactant gas and the driver gas to rest, as indicated by a contact surface separating two gases turning into a vertical line. The arrival of the primary shock wave at the endplate, where the reactive gas volume is confined by the endwall, marks the beginning of the reaction. The reaction time (the time during which the reactant gas is heated by the shock wave) is on the order of milliseconds for practical rotor speeds and may be prolonged by adjusting the rotor speed, rotor length, and flow conditions. The reaction continues until the opening of the driven gas exit port. When the exit port opens, an expansion wave (dashed-dotted line) is generated from the lower corner of the exit port propagating to the left, reducing the processed gas (e.g. products) temperature. The reaction time onboard the rotor is terminated after the processed gas is expelled from the end of the channel by the cooling action of the expansion wave. By closing the product exit port, a compression wave is generated from the upper corner of the exit port propagating to the left and stopping the channel flow. At this very moment, the fluid trapped in the channel consists to a large part of the driver gas and a very small portion of the product, preventing the driver gas from reaching the product exit port or contacting the right endplate. Closing the driver gas inlet port is timed with the arrival of the reflected shock wave and expansion wave fronts to the channel left end. Opening the driver gas outlet port creates another expansion fan from the leading corner of the outlet port which aids to scavenge the remaining of the driver gas from the downstream end of the rotor. By opening the driven gas entry port, the reactant gas

entering the channel from the left is separated by a contact surface from the expanded driver gas leaving the channel from right, i.e. an overlap process. While the overlap process continues, the scavenging of gas through the exit port is stopped by closing the port. The closing of the exit port is timed with the arrival of the driven gas to the right end of the channel. Closing the exit port generates another compression wave propagating to the left stopping the reactant gas flow. When the compression wave meets the upper corner of the driven inlet port, the port closes leaving the channel fully filled with pre-compressed reactant gas and the next cycle can be initiated. With steady rotation of the channels and a cyclic sequence of events occurring in the reformer, continuous production of hydrogen can be attained (even without cooling), greatly exceeding the single channel and rapid timing in a typical chemical shock tube [29].

3.1 Short Versus Long Residence Time

Uncatalyzed thermal methane cracking can take place above 1000^0C with sufficient residence time [30]. Nevertheless, at this temperature, the conversion and kinetics of the reaction are rather low. Studies show that around 1200^0C, the full conversion of methane into hydrogen is theoretically feasible. Temperatures above 1400-1500^0C are more ideal for shorter residence times [10, 30]. Hydrocarbons are thermodynamically unstable at such high temperatures and the methane molecule is the most resistant to decomposition, thus the intermediate products will be decomposed before the methane is. With sufficient residence time, the only products anticipated are hydrogen, carbon, and any unreacted fraction of methane. Figure 4, from Ref [10], shows the conversion of methane across a range of temperatures at atmospheric conditions. As an illustrative example, the graph predicts that approximately three milliseconds of residence time would be required at 1860^0C temperature to achieve a 40% conversion. Similarly, at a lower temperature of 1500^0C, a longer reaction time of approximately 15 milliseconds is required to obtain the same yield. In a wave reformer, temperatures in excess of 2000^0C can be generated behind the reflected shock wave, but in practice the peak temperature in the reaction zone decreases sharply because the methane-pyrolysis reaction is endothermic with heat consumed and temperatures decreasing as the reaction proceeds. Thus, at a lower temperature, a longer residence time is required in the device to maintain maximum yield of hydrogen. Ideally, this reaction time can be changed by adjusting the rotor speed, the rotor length, and port conditions. However, the rotor speed and the position and width of the ports must also be set to modulate the speed of the propagating waves in order to avoid undesired flow phenomena in the device [31]. Thus, there may be trade-offs in designing a well-tuned wave pattern. NWH_2 has developed several reformer designs that produce novel wave cycles with a goal toward promoting longer residence time and a higher fuel-to-hydrogen conversion. A selection of these designs along with prior work by others are introduced and described in the following sections.

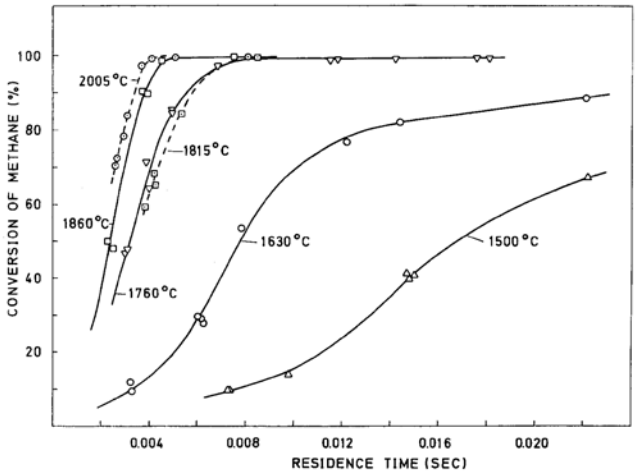

Figure 4: Methane conversion at different temperatures, adapted from Ref. [10].

3.2 Hertzberg's Wave Cycle Using a Reflection Endplate

A wave cycle that allows gas at high temperature to remain in the channel for a longer period of time was proposed and investigated by Hertzberg and his coworkers [25, 26]. It is a four-port wave reformer schematically shown in Fig. 5. The reactant gas inlet port is arranged at the right end of the chemical reactor opposite to the driver gas inlet and outlet ports and the process gas (reaction product) outlet port located at the left end of the reactor. Therefore, the rotor experiences a through-flow pattern by the reactant gas and a reverse-flow pattern by the driver gas (i.e. composite wave cycle).

The cycle starts at the bottom of the figure where preheated low-pressure reactant gas is flowing into the channel from the right inlet port while the high-pressure driver gas starts to enter from the left through opening the driver inlet port. The impact of the driver gas upon the reactant gas generates a traveling shock wave toward the right endplate. As it moves, the shock wave heats and compresses the gas, setting it in motion in the direction of the shock wave. By the time the shock wave reaches the channel right end, the reactant gas port closes. The shock is reflected from the endplate back toward the channel left end. At this moment, the reactant gas has been compressed and heated both by the primary and reflected shock waves to the selected conditions under which the reaction takes place near to the reflecting endplate. Following a further rotation of the channels, the driver gas inlet closes and the flow of driver gas into the channel is cut off. This generates an expansion wave following the shock wave, cooling both gases as it passes along the channel. The maximum temperature attained by the process gas will start to decay shortly after the expansion wave passing through the heated reactant gas strikes the right endplate, and an expansion wave is reflected upstream. The subsequent passage of the expansion waves through the reactant gas rapidly cools the reacted gas which "freezes" the high-temperature reaction products. Opening the driver gas outlet port is timed with the

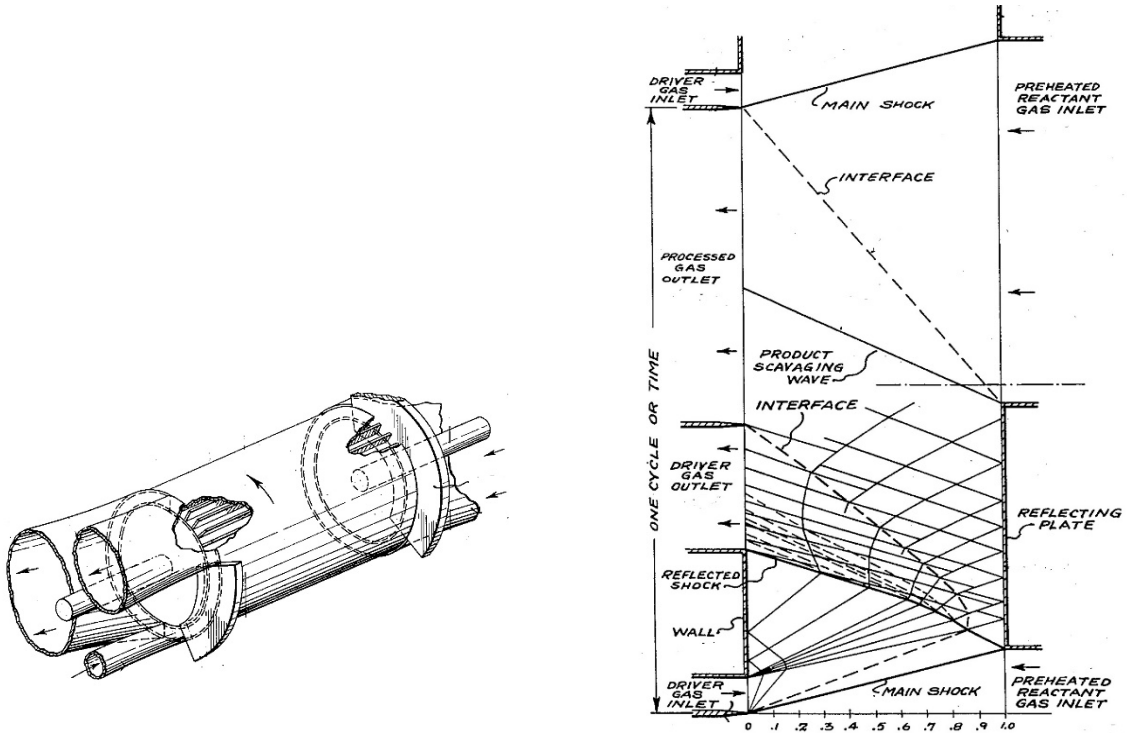

Figure 5: Four-port wave reformer concept introduced by Hertzberg et al., adapted from Ref. [25].

arrival of the reflected shock wave. When the outlet port opens, the combined effect of the expansion waves and the reflected shock wave propels the discharge of driver gas out of the channel. The outlet port closes just as the final volume of driver gas is expelled from the channel. This full evacuation of the driver gas allows the processed gas to expand to its original volume in the channel. The rotation of the channels produces steady stream of spent processed gas exiting the channel through its corresponding outlet port. Finally, admission of fresh unprocessed gas via opening its port at the right end of the channel pushes out the processed gas, thus aiding the scavenging process. The processed gas outlet port remains open long enough to complete the scavenging of the processed gas. The discharge process is finished when the interface separating the two gases arrives at the upper corner of the processed gas outlet port (which is also the lower corner of the driver gas inlet port), thereby completing the cycle. Comparing wave diagrams in Figs. 3 and 5, it will be noted that the reflecting plate in Fig. 5 has a greater circumferential extent than the similar wall in Fig. 3, allowing for the reaction products to remain longer time in the reactor which in turns produces a higher fuel-to-hydrogen conversion.

Figure 6 illustrates how this wave reformer was used to produce NO and combine it with water to produce nitric acid (HNO_3) as a final product [24]. The cycle consists of two major parts: (i) driver section, and (ii) reaction section. The driver section (left) is designed to provide hot high-pressure driver gas to carry out the compression process in the wave reactor. In this section, air enters a compressor driven by a turbine which is partially driven by a motor. The compressed air is directed to a heat exchanger where it picks up heat and then is directed to a combustion chamber. In the combustion chamber the preheated compressed air and fuel mixture is combusted to provide a high-temperature high-pressure combustion driver gas for the wave reactor. After the driver gas has expanded within the wave reactor, the low-pressure exhausted driver gas is discharged into the heat exchanger in which some of the heat of the discharged driver gas is given up to the compressed air leaving the compressor. The cooled driver gas after leaving the heat exchanger is directed to the turbine wherein the energy of the driver gas is utilized to drive the turbine. The driver gas is finally discharged from the turbine to the atmosphere.

On the reactant gas side, the reactant gas (air) is preheated through a heat exchanger after being raised to an appropriate pressure by a compressor. The preheated reactant gas then enters the wave reactor opposite from the end at which the driver gas inlet and outlet ports are located. After the reactant gas is processed within the reactor, the heated processed gas enriched with NO is discharged to the heat exchanger where it transfers some of its heat to the reactant gas entering the reactor. The cooled processed gas leaving the heat exchanger is directed to a secondary compressor to raise the gas pressure before entering an absorption tower. Water is injected and mixed with NO in the tower where HNO_3 is produced and collected from the bottom of the tower. The remaining gas is directed to a secondary heat exchanger and a turbine which drives the two compressors used in the reaction gas section of the cycle.

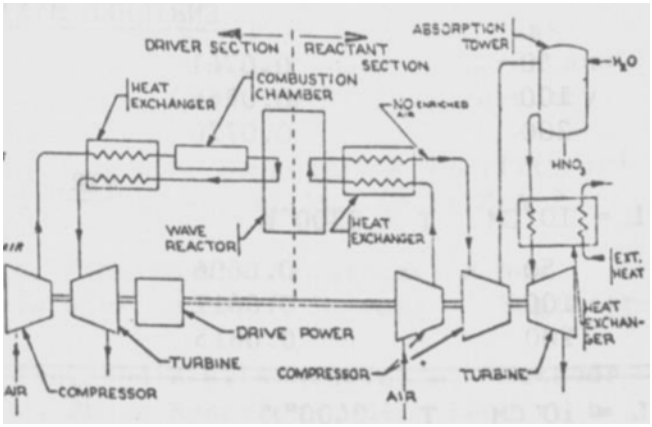

Figure 6: Schematic of a cycle designed to produce nitric acid, adapted from Ref. [24].

While this combustion-driver wave reactor system was a novel approach leading to higher reaction temperatures, the main problem area in the cycle was in the driver section which was complicated and far too inefficient. According to Hertzberg [24], the cycle suffered from a number of losses and excessive energy created by the driver circulating loop and the heat exchanger which resulted in excessive capital costs. The complexities and inefficiencies of the system prevented this approach from competing with other known nitric acid formation techniques. It is in light of these difficulties that an alternate approach, known as the fly-wheel driver concept [27, 32], was later introduced modifying the wave cycle to allow the driver gas to be removed at a total pressure slightly higher than upon entry of the reactor while the reactant gas is expanded and cooled. In this unconventional concept, the role of the driver gas and the reactant gas to be interchanged differently where the energy gain in the driver gas was made up by a corresponding energy loss in the reactant gas. Thus, in the new system, capital cost could be saved [27] through the elimination of the driver gas prime mover, turbine, compressor, heat exchanger, and combustion chamber shown in the driver section in Fig. 6. In other words, the driver section does not need a compressor, heat exchanger, and a turbine to recirculate the driver gas to the reactor. Figure 7 schematically shows a representation of this modified cycle (left) along with calculations conducted by Hertzberg et al. [32] at various states in the wave diagram (right). In this modeling, the

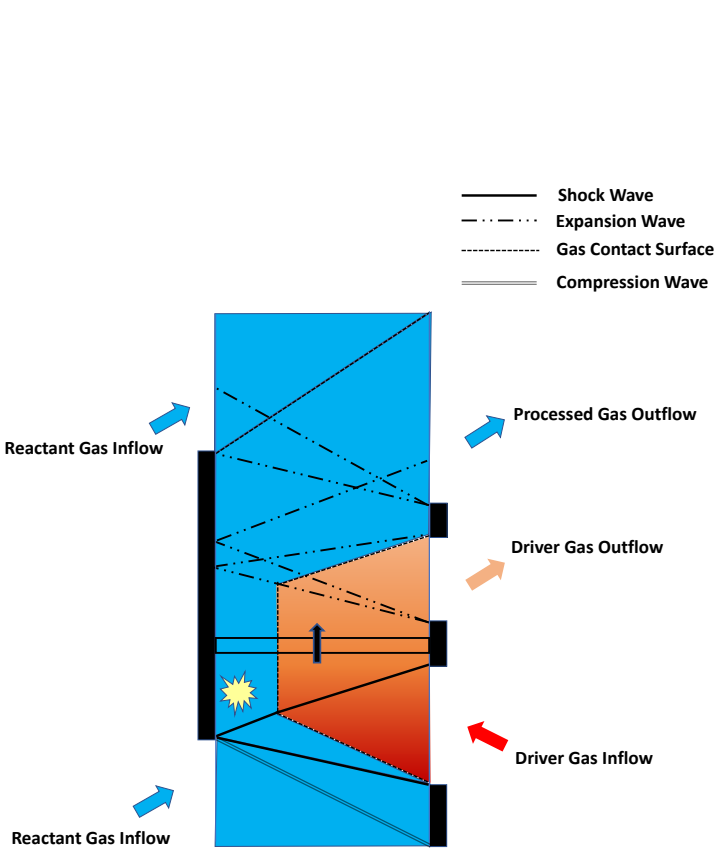

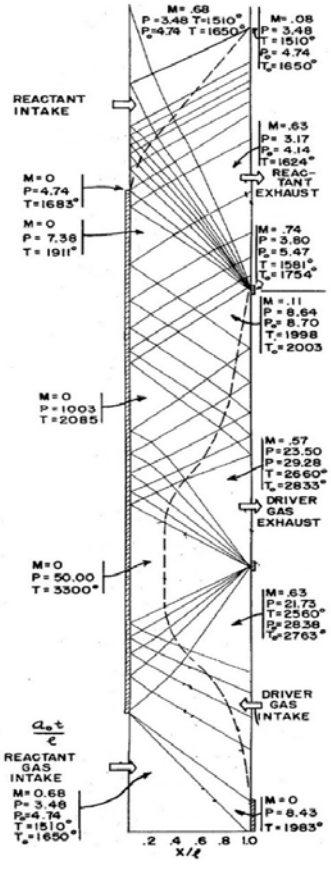

Figure 7: Wave reformer using the fly-wheel driver concept: (left) schematic wave diagram, (right) calculated flow properties, adapted from Ref. [32].

reactant and driver gases were both nominally chosen to be air. The temperatures are given in degrees Kelvin, and the pressures in atm. To initiate the cycle, at the bottom of the figure, preheated reactant air enters the channel from the left via its inlet port at a Mach number of 0.68 and static pressure and temperature of 3.48 atm and 1510 K, respectively. The reactant gas is brought to rest by a hammer shock generated by the right endplate, which raises the pressure in the channel and brings the reactant gas completely to rest. The reactant gas is further pressurized by opening the channel to the driver gas inlet port from the right carrying out a driver gas at a Mach number of 0.64 and static pressure and temperature of 21.73 atm and 2560 K, respectively. The dashed line in this drawing represents the interface between the reactant and driver gas during channel filling by the driver gas. Notice that the contact surface becomes motionless (vertical line in space-time) when the reflected shock wave hits it. The reaction conditions are met near to the reflecting wall at about 50 atm and 3300 K. Comparing Figs 7 and 5, it is seen that closure of the driver gas inlet port is delayed for the modified cycle eliminating the expansion wave seen at the upper corner of the inlet port in Fig. 5. Thus, the driver gas is expanded to static pressure and temperature of 23.50 atm and 2660 K, respectively, only once by an expansion wave initiated through opening the driver outlet port after allowing the appropriate time for the reaction to occur. The driver gas exhaust pressure is slightly above the driver gas inlet pressure, allowing recirculation of the driver without the need for auxiliary pumping system, i.e. a self-driven wave machine. The expansion wave passes through the driver gas, crosses the interface between the processed gas and the driver gas, then passes through the processed gas and begins to accelerate the processed gas back toward the driver exhaust end of the channel as the driver gas flows out of the channel. The expansion wave is then reflected from the left endplate which reduces the processed gas temperature further. The reactant product is scavenged, after the driver gas completely leaves the channel, through opening the processed exhaust port. This initiates another expansion wave that cools the processed gas even further to a temperature (1504 K, not shown) slightly below the reactant intake temperature without destroying the NO produced. The reactant gas exhaust pressure (3.17 atm) also drops below the reactant intake pressure. Therefore, the reactant gas expands across the reactor through at least three expansion waves while the driver gas is only affected by one expansion wave. Finally, the scavenging process continues while the expansion wave assists to bring in the fresh charge of reactant from the left. The remaining processed gas is further removed with the introduction of fresh unprocessed gas, thus arriving at the same gas conditions to repeat the cycle.

3.3 Hertzberg's Wave Cycle Employing Head-On Colliding Shock Waves

In wave diagrams described in Figs. 5 and 7, the peak temperatures and pressures occur adjacent to an endplate where the shock waves are reflected from the wall. Allowing the shock wave to reflect from a rigid wall is an effective way to create very high temperature, but excess heat transfer to the endplate over a long period of operating the reformer could be a serious problem. Additionally, because the channels are spinning at a high speed and the endplate is stationary, the seal between the stationary endplate and the channels could suffer from high temperatures and pressures in that region. To avoid this problem, Hertzberg et al. proposed an alternative cycle that eliminated the need for a seal at the region where the high temperatures and pressures occur in the reactor [26, 27]. In this new proposed cycle, the reaction zone is designed to be placed in an intermediate or middle section of the channel, thereby the region of high temperature and pressure occurs in the central portion of the process gas column and not at an end which must be sealed against a reflecting plate. This can be done by simultaneously introducing opposing pairs of shock waves at opposite ends of the channels. This design is schematically illustrated in Fig. 8 where a six-port wave rotor (top) is envisioned through use of a so-called "double-ended" type wave diagram within the reactor (bottom). In fact, reflecting a shock wave from a plane wall is analogous to the head-on collision of two shock waves of equal strength [33]. This has been also experimentally verified in a double shock wave tube where head-on collisions of identical shock waves of the gases Ar, Xe, CO_2 for instance Mach numbers from 1 to 10 were produced and studied [34]. Recent numerical modeling of shock tubes with opposing incident shocks in wet steam flows have also been reported [35]. Thus, the wave diagram shown in Fig. 8 is expected to provide a similar heating process for the reactant gas comparable with that in the cycle described in Fig. 5 (or Fig. 7) without wall-effects.

In Fig. 8, each cycle consists of three inflow ports where ingress of the fresh driver and reactant fluids are fed into the moving channels, and three outflow ports where processed (product) and spent driver gases are discharged from the rotor channels. The process begins at the bottom of the wave diagram where the fresh preheated reactant gas is charged into the upstream end of the channel via an intake port while the processed reactant gas (e.g. product) is being discharged from the downstream end of the channel through an exhaust port, e.g. an overlap process in which both channels ends are open. When the entire channel is filled with the fresh reactant gas, the exit port closes. Upon closing the exit port, the reactant gas is brought to rest and its pressure is raised. When the hammer shock meets the upper corner of the inlet port, the ingestion of the fresh gas into the channel is stopped. At this instance, the channel is fully filled with compressed fresh reactant gas. As the channel rotates further, the channel ends are exposed to high-pressure driver gas entry ports and opposing pairs of shock waves are triggered from the lower corners of the inlet ports. These opposing shock waves cause a sudden rise of pressure and temperature inside the channel. Behind the primary shock waves, the compressed reactant gas and the driver gases are separated through two contact surfaces as the compression process is carried out. These contact surfaces (showing the progression of the two fluids) follow the shock waves at slower rates. The two shock waves symmetrically collide in the middle of the channel and leave as a pair of reflected shock waves. When two shock waves collide, the effect is the same as though there were a solid reflecting wall

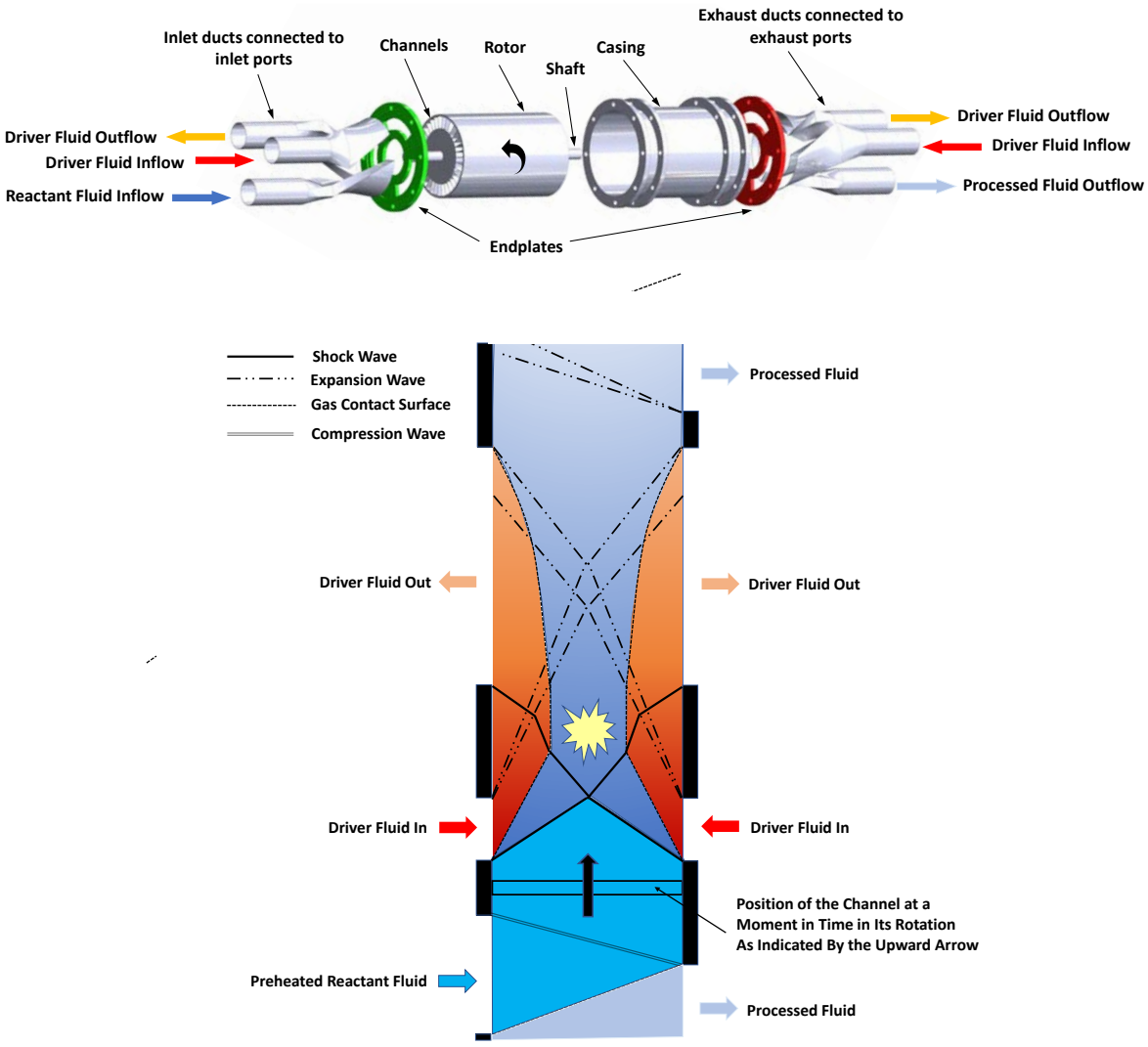

Figure 8: Six-port wave reformer (top), employing opposing pairs of shock waves (bottom).

at the plane of impact, similar to the condition previously shown in Fig. 7, with the added benefit of reducing the overall leakage of the device. The pressure and temperature of the reactant gas in the reflection zone behind the reflected shock waves rise further, and the double-compressed gas is brought to rest (as indicated when the contact surfaces turn into vertical lines). With sufficient compression by the primary and reflected shock waves, thermal dissociation of the methane to hydrogen can occur in the motionless heated zone behind the reflected waves. Meanwhile, the driver gas entry ports start to close, generating expansion waves in opposing pairs from opposite ends of the channel. The duration of the peak temperature is limited by the arrival of the expansion wave fronts. The expansion waves rapidly cool the reaction products, and then leave the center of the channel traveling toward opposite ends. Discharging the spent driver gas starts with the opening the driver outlet ports which is timed to coincide with the arrival of the reflected shock waves. Then, the closing of the outlet ports is timed to coincide with the arrival of the expansion waves. By the time the expansion waves arrive at the channel ends, the entire volume of spent driver gas has left the channel and the channel is entirely filled with the processed gas. Finally, decomposed gas (e.g. hydrogen and any intermediaries) is expelled from the channel by another expansion wave generated from the leading corner of this exhaust port. Opening of the driver gas port is timed with the arrival of the expansion wave to the left end of the channel to allow fresh reacting gas to enter the channel and the cycle repeats itself.

Lauer et al. [36] built and demonstrated methane pyrolysis in a single-channel shock wave reformer using the head-on colliding shock waves. Their unconventional disk-shape apparatus consisted of a shock tube that would rotate within a

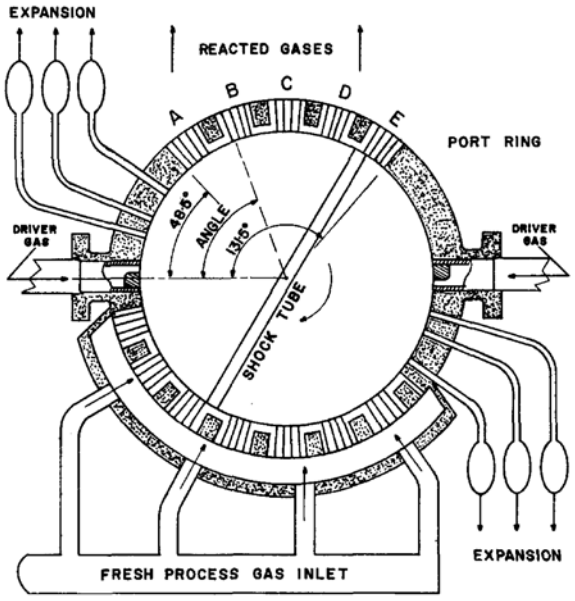

Figure 9: Disk-like shock wave reformer, adapted from Ref. [36].

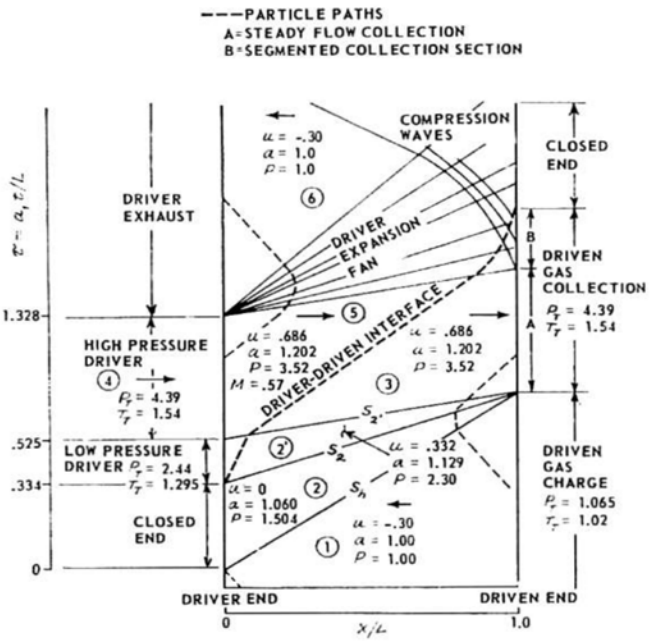

Figure 10: Wave diagram for a four-port wave rotor with staged compression, adapted from Ref. [20].

stationary ring with two complete cycles of operation per one revolution of the disc, as shown in Fig. 9. The driver and driven gas intake/outlet ports were located in the ring with approximately 0.02 inch clearance around the disc, except at the driver gas inlet ports where they are adjustable to <0.001 inches. Fresh process gas flows into the system to expel the reacted gas and to refill the tube in the center of the ring. When the tube is at horizontal position, the opposite ends of the tube connect to the reservoir of high-pressure driver gas. The driver gas then enters the tube from each end, creating two shock waves that collide and reflect. The driver gas expands and exists the tube through three expansion ports. This allows the gradual expansion of the spent driver gas and partial pressure recovery. Experiments using 1% of either butane, hexane, methane or cyclohexane feedstocks and 99 % Ar demonstrated pyrolysis of each compound. Test times ranged from 0.04–0.10 milliseconds, at rotational speeds between 3000-7000 rev/min, resulted in reflected shock pressures up to 45 bar and temperatures up to 2000 K. These experiments demonstrated that the degree of conversion (cracking and decomposition) increases with molecular weight which was consistent with published studies of hydrocarbon pyrolysis in classic shock tubes. To the authors knowledge, this is the only reported experimental work that revealed large quantities of reaction products with a single-channel wave reformer.

4. WAVE REACTOR USING STAGED-SHOCK COMPRESSION

The main feature of the wave cycles introduced by Hertzberg et al. was to superheat a reactant gas by shock compression and to maintain it long enough to promote equilibrium formation of NO followed by immediately cooling the reaction gas product by expansion waves to preserve the desired equilibrium. However, rapid cooling has a negative effect in conversion of hydrocarbon fuel to hydrogen in methane pyrolysis due the preferred benefit of longer reaction time at high temperatures. For the NWH_2 application, cooling the processed gas will likely be deliberately avoided to promote higher hydrogen conversion values. NWH_2 has proposed a new wave cycle design that benefits from staged-driver compression (where at least two driver gas ports are used for elevating the peak temperature) and longer time at high temperatures (allowing the processed gas to remain at a high temperature at exit instead of expanding the gas as in the previous cycles).

The notion of staged compression has been pursued by several researchers [20, 37]. It is well recognized that if the number of shocks is increased for a fixed overall compression ratio, the efficiency of compression increases. One method of staging included dividing the driver gas inlet port into two segments (e.g. using a partition), connecting the first section to a low-driver supply and the second part to a high-driver reservoir pressure. This is shown in the wave diagram in Fig. 10 where a four-port pressure-exchange wave rotor is used to energize a driven gas using two stages of compression (the entire cycle is not shown by the authors). Here, the wave rotor operates on a reverse-flow wave configuration where the gas streams enter and leave the channel from the same end. In this cycle, first the driven gas is compressed by the hammer shock (S_h), then it is compressed further by using a two-stage driver port. The first

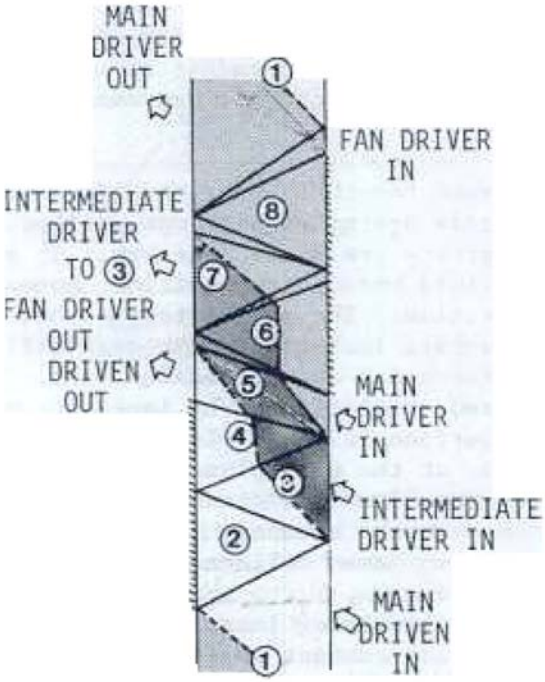

Figure 11: Wave diagram for MSNW's wave rotor with staged compression, adapted from Ref. [37].

incidence shock wave (S_2) is generated by the low-pressure driver stage and the high-pressure driver stage initiates the second incidence shock wave ($S_{2'}$). An overall compression ratio of the driven gas of 4.39 is obtained through these three shock waves. By increasing the number of compression stages, a more efficient pressure-exchange process between the driver and driven gases could be achieved, but it would demand an extensive ducting system which may not be practical. Mathematical Sciences Northwest, Inc. (MSNW), designed and tested a pressure-exchange wave rotor with 2.5 pressure ratio between its driver to driven gases [38] introducing a wave cycle that used multiple-driver stages to ultimately achieve a high-pressure ratio of 5.6. This latter pressure ratio was in the range of interest for energy-exchanged applications towards the advanced power system cycles they were exploring. Figure 11, from Ref. [37], schematically illustrates their wave diagram where the driven gas is compressed with a few shock waves created by driver gases at different entry pressures.

Here, a new wave cycle employing multiple driver ports is proposed where at least two separate driver gas ports are used, as schematically shown in Fig. 12. In this arrangement the endplates are provided with three inflow ports and three outflow ports. This new six-port wave reformer allows the reactant gas to enter and leave at the same end of the rotor (on the left-hand side of the diagram) via inlet and exhaust ports, but driver gases are being fed into and expelled out of the rotor twice through their

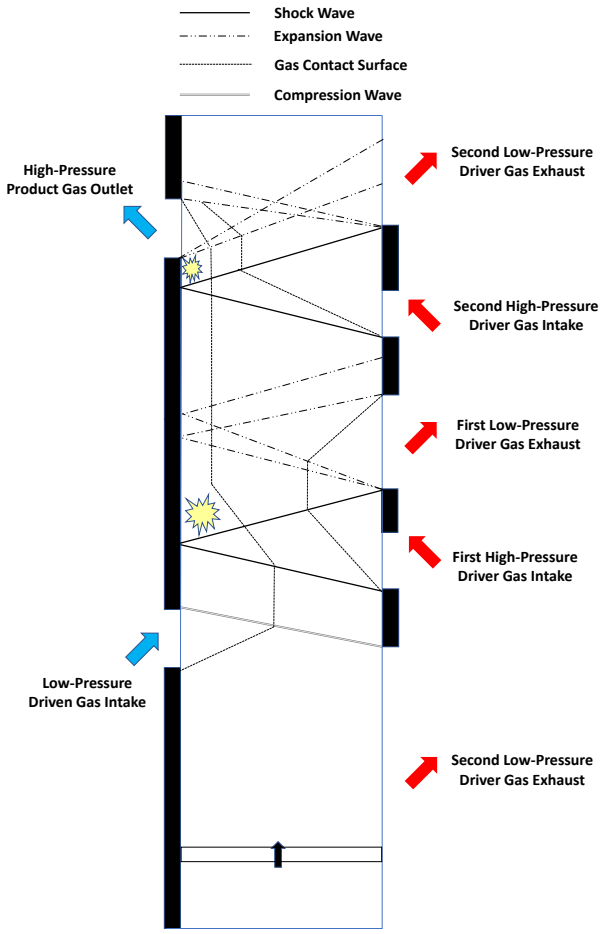

Figure 12: Simplified wave diagram for a dual-driver port wave reformer.

corresponding entry and exhaust ports at the opposite end of the rotor (on the right-hand side of the diagram).

The cycle starts from the bottom of the picture when the channel filled with driver gas from a previous cycle is opened to a low-pressure outlet port. Then, fresh reactant gas enters the channel via an inlet port on the left side of the channel. This fresh gas is separated from the driver gas by a contact surface. When the exhaust port closes, a hammer shock is generated from the upper edge of the port that travels toward the inlet port stopping the channel flow. As the wave reaches the upper corner of the inlet port, the inlet port closes. At this moment the channel is partially filled with the fresh reactant gas and the remaining portion of the driver gas in the channel (e.g. residual gas). By opening the first driver gas port, the first driver gas compresses the residual driver gas and the fresh reactant gas through a primary and a reflected shock wave in the first stage. This heating process provides suitable reaction conditions in the first reaction zone behind the reflected shock wave and adjacent the left endplate. The first driver gas starts to expel from the channel's right end by opening another driver gas exhaust port.

Expansion waves generated at the downstream end propagate upstream toward the hot reaction zone facilitating a scavenging action for the driver gas. These expansion waves pass through the heated reactant gas and reflect at the closed upstream end. By closing the exhaust port, the first driver gas is fully scavenged and the heated reactant gas adjacent to the left endplate is carried out by the channels. After allowing the appropriate time for carrying out the heated reactant gas, the next (second) phase of compression starts. Similar to the shock-heating process in Fig. 3, the right end of the channel is exposed to a secondary driver gas port. Another set of incidence and reflected shock waves creates a secondary reaction zone forming behind the secondary reflected shock wave. The processed gas leaves the channel through the outlet port placed at the left endplate. The port remains open long enough to complete the scavenging of the processed gas. This scavenging is also facilitated by an expansion wave generated at the lower corner of the outlet port. At the right end of the channel, another exhaust port opens and an expansion fan originates from the leading edge of the exhaust port and propagates upstream into the channel expanding and discharging the secondary driver gas to the surrounding and the cycle repeats.

4.1 Numerical Modeling

The numerical tool used for modeling in this paper is developed by Tüchler and Copeland in conjunction with their wave rotor studies at University of Bath, UK. Details of the code including algorithm, numerical approach, loss modeling, and boundary condition implementations have been described in previous publications [13, 39], thus, only a brief description is provided here.

The code follows a single channel of the wave rotor, as it rotates past the various ports. The aspect ratio (e.g. length to width ratio) of the wave rotor channels is assumed to be sufficiently large for the flow to be treated as one dimensional. Thus, the code assumes that all quantities are uniform across the channel cross section as functions of time. This quasi one-dimensional (Q1D) numerically integrates the mass, momentum, and energy equations for a calorically imperfect gas, solving the laminar Navier-Stokes equations using a two-step Richtmyer time variation diminishing (TVD) scheme. The model accounts for wall heat transfer, flow leakage, wall friction, and leakage between the channels and endplates. Inflow losses due to incidence, and channel gradual opening/closing are also accounted for in the code. Q1D uses an input file which contains a number of non-dimensional terms that describe the port size, channel size, rotor length, rotational speed, cycle length, endplate gap(s), etc. Port pressures and temperatures set by the user are used as boundary conditions. Using this code, the port mass flow rates, port sizes, and their arrangements will be optimized. Since its development, the code has been successfully used in the simulation of a micro gas turbine that employed a wave rotor turbine with cambered channels at University of Bath. The model was furthermore validated through both literature data and experimental data from a symmetrically cambered micro-wave rotor for shaft power extraction. Q1D is recognized as an inexpensive design tool that can be used for initial sizing before more expensive numerical modeling tools are applied. The code has been recently modified to use dissimilar driver and driven gases and to account for onboard reaction. Details of these modifications will be discussed in a future publication.

Figure 13 represents a numerical modeling of a NWH_2 wave reformer incorporating the wave cycle details discussed above. Preheated methane is used as the driver and the driven gases. The terms “HP” and “LP” refer to high pressure and low pressure, respectively. The color contours show non-dimensional pressure, temperature, Mach number, velocity, and molar fraction of methane and hydrogen in a representative channel, as a function of time (vertical axis) and position (horizontal) over one complete cycle of operation. A color scale bar is provided to the immediate right of each contour plot. Axial distance is non-dimensionalized by channel length, L. Vertical axis represented by angular displacement, θ, is non-dimensionalized by maximum angular displacement, θ_{max}, which is 360 degrees. The pressure and temperature are non-dimensionalized by the driven inlet port stagnation state properties, respectively. The velocity is non-dimensionalized by the maximum gas velocity in the channel which corresponds to the velocity of incoming flow at the first driver inlet port.

Starting from the temperature plot, it shows the inward movement of the contact interface between cooler gas in the channels and preheated fresh reactant gas received at the inlet port at non-dimensional time 0.3. Along with the pressure plot, a region of high-pressure is seen after opening the first driver inlet port at non-dimensional time 0.45 due to compression by the incidence shock wave. A more significant higher-pressure high-temperature region near to the left endplate is also seen where a reflected shock wave is created. The temperature plot also indicates a region of high temperature at non-dimensional times between 0.45-0.62 with a peak temperature of 1440 K approximately three times higher that of the driven inlet port stagnation temperature. This peak temperature and channel pressure decrease considerably after opening the corresponding outlet port at non-dimensional time about 0.58 due to the gas expansion. The temperature plot also shows the second stage of compression starts at an initial temperature higher than that in the low-pressure methane intake port (dark blue), indicating the first stage of compression preheats the channel gas prior to shock heating in the second stage. The processed gas leaves the channel from its corresponding outlet port, which opens at non-dimensional time 0.8 (left), at a relatively high temperature and high pressure. On the pressure plot, the incidence and reflected shock wave trajectories are clearly seen in both stages of compression with highest gas pressures represented by dark red colors. For stability reasons, in these preliminary simulations, the partial opening/closing feature of the code was not activated, i.e. the channel is considered to open and close instantaneously as it passes through the ports. Thus, the incidence shock waves are created only a short time before the driver intake ports open. The depression of pressure (light red) due to the generated expansion

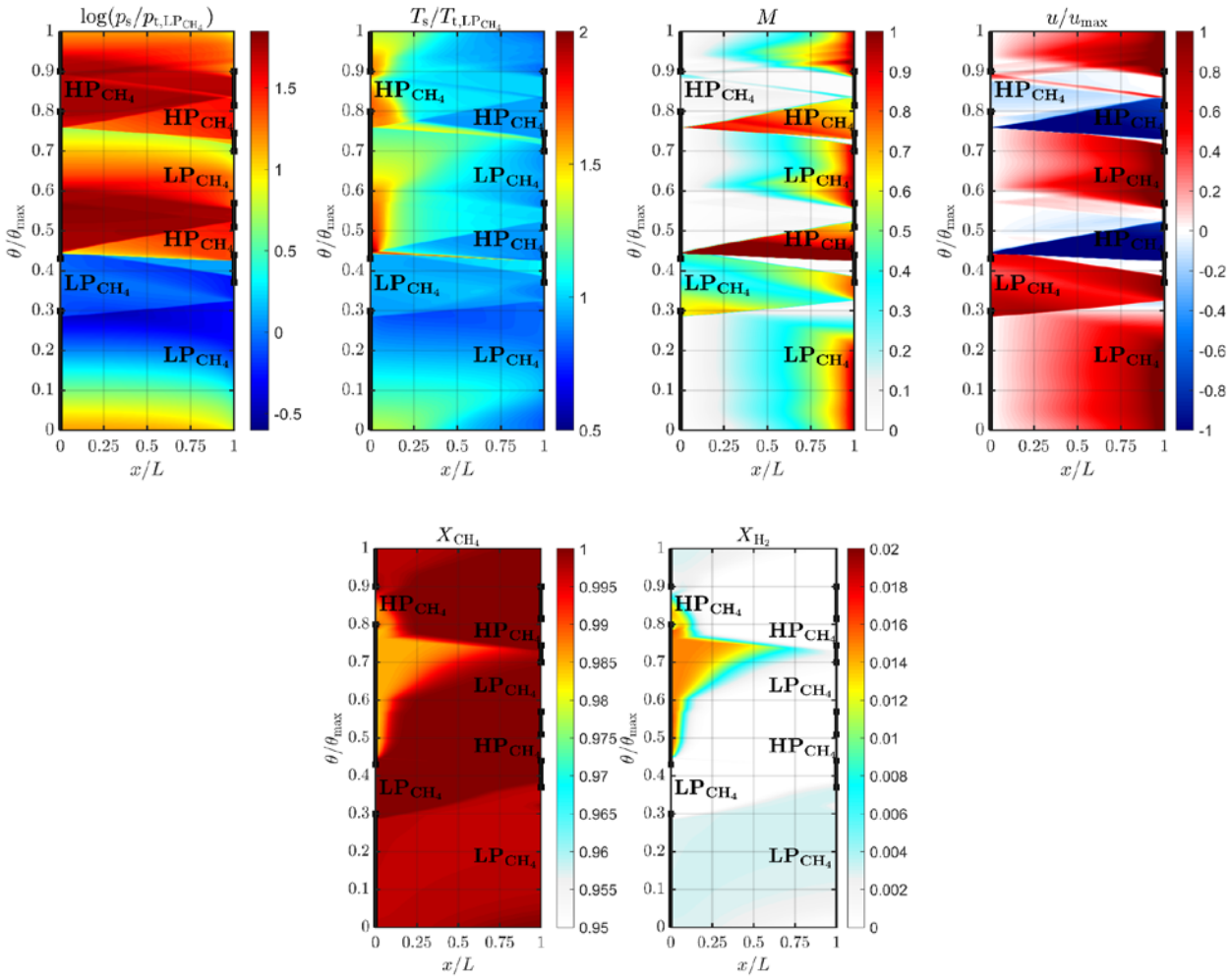

Figure 13: Contours of non-dimensional pressure, temperature, velocity, Mach number (top), and molar fraction of methane and hydrogen (bottom) in a dual-driver port wave reformer.

fans are seen at non-dimensional times about 0.58 and 0.9 (right) for the first and second stages of compression, respectively.

The velocity plot shows how the reactant gas is stopped by the hammer shock when the driver outlet port closes at non-dimensional time about 0.38 where the gas velocity goes to zero after it encounters the endplate (white color). Shortly after, the velocity of incoming driver gas goes to zero as well near to the left endplate by the first reflected shock wave at non-dimensional time about 0.45. The heated gas after the first stage of compression remains in the channels adjacent to the left solid wall until it is heated again by the second stage of compression. Regions of zero velocities are seen near both endplates throughout the entire cycle. The Mach number contour shows choked conditions for the entire portions of the driver inlet and exit ports in the first stage of compression and the flow remains sonic for most portions of the driver exit port in the second stage of compression. The region with the highest Mach number is just behind the first incidence shock wave, where the shock strength is highest compared with other shock waves in the cycle.

The molar fraction plots (bottom of Fig. 13) illustrate distribution of methane (reactant gas) and hydrogen as product in the reformer. The methane contour shows filling of the channel by methane through driver and driven intake ports. Conversion of methane to hydrogen starts when the driven inlet port closes and continuous as the reaction is carried. Upon exhaust opening of the product, the entire produced hydrogen is not completely purged, and some hydrogen (light turquoise) remains in the channel and carried over to the next cycle.

These preliminary numerical results demonstrate that the proposed wave cycle can be used to crack methane and produce hydrogen. It is acknowledged that for a more accurate simulation of the flow field inside the reformer, a detailed modeling (e.g. two- or three-dimensional predictions) is essential to capture all fluid phenomena such as turbulence and mixing. This 2-D and 3-D modeling, along with iterative lab and field prototype validation, and detailed kinetics studies are part of the current NWH_2 development program. These simulations and data will be important in designing a wave reactor capable of high

conversion rates of hydrogen from methane cracking where shock temperature and duration are key optimization parameters. Much can be learned from a well-instrumented experimental rig. A single-stationary channel with rotating endplates to simulate a wave reformer with only one channel is foreseen as the simplest configuration. Single-channel experiments can demonstrate the operation of actual wave reformers, but in a less complicated architecture. This design may be preferred for laboratory investigations and has been demonstrated [40-43] to create an opportunity to experimentally measure or visualize flow measurement in the channels. It is well-recognized that such a configuration has more than one rotating part and sealing becomes more complex, therefore this arrangement rarely seems to be convenient for commercial purposes. The NWH_2 team has designed and built a single-channel wave reformer that is being used in the current program tests. The success and results of these tests will be used to design and build a multi-channel wave reformer capable of producing environmentally friendly hydrogen on an industrial scale.

5. CONCLUSION

This paper introduced and discussed a method for continuously processing reactant gas by the successive action of compression and expansion waves to produce hydrogen, in a wave rotor. For over 50 years, wave rotors have been successfully utilized in power generation, propulsion, automobiles, chemical processes, refrigeration, and other applications. Today, wave rotors are perhaps most frequently associated with performance-enhancement of stationary power gas turbines or aeropropulsion engines. However, their use is not limited to gas turbine engines. From the early 1950's to today, wave rotors have also been used as a chemical reactor and pyrolizer. Cornell Aeronautical Laboratory successfully operated a CAL Wave Superheater for over a decade in the late 1950's and 1960's. The Wave Superheater was designed to compress and heat air to temperatures greater than 3500 K and up to 120 atm. Subsequent work led to refinements in the ability to simulate continuous production and a range of novel designs and wave cycles. Hertzberg and colleagues were pioneers in this, exploring composite wave cycles designed to prolong residence times and various designs that used colliding shock waves with double compression zones intended to increase peak temperatures.

A single channel in a wave rotor is analogous to a classic shock tube, both use unsteady waves to transfer energy. In a shock tube the rupture of diaphragm initiates the shock wave. Similarly, in a wave rotor the opening of the end ports initiates the wave cycle. However, one of the advantages of the wave rotor is the flexibility in design parameters (e.g., valve or port timing, number of ports, port size and angle, drum size, drum rotational speed). This allows the design of a wide variety of gas interactions (wave cycles), configurable to support many different applications.

This paper describes the evolution of select wave rotor designs through prior decades of research and describes recent adaptations proposed for evaluation in the ongoing development of a wave rotor-based methane pyrolysis technology (i.e., the NWH_2 Wave Reformer).

As with other wave rotors, the wave reformer uses shock waves to transfer energy between two compressible fluids such that a driver gas expands and a driven gas is compressed. Although this is similar to a shaft-coupled gas compressor and turbine, there are a number of important differences. First, a wave reformer achieves these compression and expansion cycles through the exchange of energy directly in a shock or expansion wave without the need for mechanical power transfer. Thus, the wave reformer only requires a small input shaft power to overcome windage and friction. In addition, unlike traditional turbomachinery that often suffer from losses that proportionally increase with a decrease in size, wave rotor performance is not as sensitive to scale. Thus, the unique properties of wave rotors allow the NWH_2 system to be readily scalable to both small, distributed uses and to very large, centralized applications.

In the baseline design, a driver and a driven gas are the primary inflows. In the wave reformer, these are both typically the same hydrocarbon gas (e.g., natural gas, biogas, propane, etc.) but at different pressures and temperatures. The system is designed to optimize conversion efficiency, typically by optimizing the peak temperature and residence time for the reaction. The peak temperature is, in turn, a function of the ratio of the temperatures and pressures of the driver and driven gas, both of which determine the strength, or Mach number, of the primary shock wave. The reaction time (the time during which the reactant gas is heated by the shock wave) is on the order of milliseconds and may be prolonged by adjusting the rotor speed, rotor length, and flow conditions. However, there are other limiting conditions to these adjustments due to the need to avoid instabilities.

Based on experimental results from customized shock tube tests and customized CFD modeling, the NWH_2 peak temperatures and residence times are sufficient to achieve methane thermal decomposition. In contrast to other methane pyrolysis approaches, no catalyst is required (though they may optionally be used) and the reaction is not driven by electricity or plasma heating processes. The NWH_2 reformer is designed to require very little input electricity, instead it takes advantage of the energy already embodied in a pressurized pipeline.

The current predominant method of hydrogen production globally is SMR which uses natural gas and steam in a gas-shift reaction, producing hydrogen and CO_2. This is why SMR is often paired CCS in what is termed 'blue hydrogen' production. PEM electrolysis is a predominant emerging 'green hydrogen' production method, but it is only 'green' when paired with renewable energy sources. Electrolysis has a high electricity demand and in regions with conventional (fossil-fuel) powered electricity, electrolysis can actually have a very high net CO_2 emission. In terms of GHG emission reduction, each of these predominant production methods are co-dependent on the parallel build-out of new infrastructure.

In contrast, the NWH_2 process may embody the best of each, i.e. low electricity demand and no direct CO_2 emissions, while also using existing infrastructure (natural gas pipelines) in

distributed and centralized hydrogen production. The unique attributes of wave rotors support an elegantly simple system, using proven components in a novel application. The simplicity, materials, and low energy inputs support projected low capital and operating costs.

The NWH_2 team includes the primary developers of one of the few recent, advanced CFD codes specific to wave rotors. The Tüchler and Copeland (2019 to 2021) experimentally validated CFD model has been customized to produce a 1-D code for the wave reformer. The computational models are critical to understanding the complex wave dynamics, energy transfer, and reaction processes. The models support design experimentation, sensitivity analysis, and variable optimization.

In summary, research over the past 50 years has explored the unique attributes of wave rotors and has resulted in a range of well-proven, reliable and viable commercial applications. The ability of wave rotors to heat gases to high temperatures is well-known, as is the use of shock waves in chemical reactions, including over 30 years of shock wave driven methane thermal decomposition (methane pyrolysis) studies. The authors cite relevant history and describe pioneering work in the development of complex, colliding, and reflecting wave cycles. This prior work forms a strong foundation for the recent work described in the development of a new wave reformer for methane pyrolysis-based hydrogen production. With no combustion, low electricity demand, and no direct CO_2 production, the NWH_2 process is a promising emerging technology. The ability to use existing infrastructure may also augment the future market viability of the technology. In total, the combination of attributes may help overcome known roadblocks in the hydrogen transition, stimulating demand, and accelerating a rapid transition to a low-carbon energy paradigm.

ACKNOWLEDGEMENTS

The authors would like to thank and acknowledge the co-funding for this and ongoing work from Emissions Reduction Alberta (ERA), Total Energies, the Natural Gas Innovation Fund (NGIF) and its members, GRTgaz, and The Transition Accelerator.

REFERENCES

[1] Fang, Z., Smith, R. L., and Qi, X., 2015, “Production of Hydrogen from Renewable Resources,” in *Biofuels and Biorefineries*, Springer.

[2] Mondal, K. C., and Chandran, S. R., 2014, “Evaluation of the Economic Impact of Hydrogen Production by Methane Decomposition with Steam Reforming of Methane Process,” International Journal of Hydrogen Energy, Vol. 39, No. 18, pp. 9670‑9674.

[3] Muradov, N., 2017, “Low to Near-Zero CO_2 Production of Hydrogen from Fossil Fuels: Status and Perspectives,” International Journal of Hydrogen Energy, Vol. 42, No. 20, pp.14058‑14088.

[4] Sun, P., Young, B., Elgowainy, A., Lu, Z., Wang, M., Morelli, B., and Hawkins, T., 2019, “Criteria Air Pollutants and Greenhouse Gas Emissions from Hydrogen Production in U.S. Steam Methane Reforming Facilities,” Environmental Science and Technology, Vol. 53, No. 12, pp. 7103-7113.

[5] Kumar, S. S., and Himabindu, V., 2019, “Hydrogen Production by PEM Water Electrolysis: A Review,” Materials Science for Energy Technologies, Vol. 2, No. 3, pp. 442-454.

[6] Knowlen, C., Mattick, A., Russell, D., and Masse, R., 1995, “Petrochemical Pyrolysis with Shock Waves,” AIAA Paper 95-0402.

[7] Nill, L., and Jahrmarkt, T., 1995, “Design of a Supersonic Steam Tunnel for Use as a Shock Wave Reactor,” AIAA Paper 95-0016.

[8] Bedarev, I. A., Parmon, V. N., Fedorov, A. V., Fedorova, N. N., and Fomin, V. M., 2004, “Numerical Study of Methane Pyrolysis in Shock Waves,” Combustion, Explosion, and Shock Waves, Vol. 40, No. 5, pp. 580–590.

[9] Shao, J., Ferris, A. M., Choudhary, R., Cassady, S. J., Davidson, D. F., and Hanson, R. K., 2020, “Shock-Induced Ignition and Pyrolysis of High-Pressure Methane and Natural Gas Mixtures,” Combustion and Flame, Vol. 221, pp. 364-370.

[10] Holmen, A., Olsvik, O., and Rokstad, O. A., 1995, “Pyrolysis of Natural Gas: Chemistry and Process Concepts,” Fuel Processing Technology, Vol. 42, No. 2-3, pp. 249-267.

[11] Akbari, P., Nalim, M. R., and Müller, N., 2006, “A Review of Wave Rotor Technology and Its Applications,” ASME Journal of Engineering for Gas Turbines and Power, Vol. 128, No. 4, pp. 717-735.

[12] Zehnder, G., Mayer, A. and Mathews, L., 1989, “The Free Running Comprex®,” SAE Paper 890452.

[13] Tüchler, S., and Copeland, C. D., 2020, “Validation of a Numerical Quasi-One-Dimensional Model for Wave Rotor Turbines with Curved Channels,” ASME Journal of Engineering for Gas Turbines and Power, Vol. 142, No. 2, pp. 021017.

[14] Shreeve, R., Mathur, A., Eidelman, S., and Erwin, J., 1982, “Wave Rotor Technology Status and Research Progress Report,” Report NPS-67-82-014PR, Naval Post-Graduate School, Monterey, CA.

[15] Welch, G. E., 2000, “Overview of Wave-Rotor Technology for Gas Turbine Engine Topping Cycles,” Novel Aero Propulsion Systems International Symposium, The Institution of Mechanical Engineers, pp. 2-17.

[16] Lapp, K. P., Polanka, M. D., McClearn, M. J., Hoke, J. L. and Paxson, D. E., 2017, “Design and Testing of a Micro-Scale Wave Rotor System,” AIAA Paper 2017-5030.

[17] Guzzella, L., Wenger, U., and Martin, R., 2000, “IC-Engine Downsizing and Pressure-Wave Supercharging for Fuel Economy,” SAE Paper 2000-01-1019.

[18] Weatherston, R. C., Smith, W. E., Russo, A. L., and Marrone, P. V., 1959 “Gasdynamics of a Wave Superheater Facility for Hypersonic Research and Development,” CAL Report No. AD-118-A-1, AFOSR TN 59-107.

[19] Carpenter, J., 1959, “Engineering Design of a Wave Superheater Facility for Hypersonic Research and Development," CAL Report No. AD-1118-A-2, AFOSR TN 59-108.

[20] Weatherston, R. C., and Hertzberg, A., 1967 “The Energy Exchanger, A New Concept for High- Efficiency Gas Turbine Cycles,” Journal of Engineering for Power, Vol. 89, No. 2, pp. 217-228.

[21] Glick, H. S., 1958, “Shock Tube Studies of Reaction Kinetics of Aliphatic Hydrocarbons,” Symposium (International) on Combustion, Vol. 7, No. 1, pp. 98-107

[22] Glick, H. S., Squire, W., and Hertzberg, A., 1955, “A New Shock Tube Technique for the Study of High Temperature Gas Phase Reactions,” Symposium (International) on Combustion, Vol. 5, No. 1, pp. 393-402.

[23] Rose, P. H., 1979, “Potential Applications of Wave Machinery to Energy and Chemical Processes,” Proceedings of the 12th International Symposium on Shock Tubes and Waves, pp. 3-30.

[24] Hertzberg, A., 1975, “Nitrogen Fixation for Fertilizers by Gasdynamic Techniques,” Proceedings of the 10th International Shock Tube Symposium, pp. 17-28.

[25] Hertzberg, A., Glick, and H. S. Squire, W., 1958, “Methods and Apparatus for Continuously Carrying Out Gas Reactions Which Require a High Temperature to Promote the Reaction and Rapid Cooling to Preserve the Reaction Product,” U.S. Patent Number 2,832,666.

[26] Glick, H. S., Hertzberg, A., Squire, W., and Wetherston, R., 1959, “Methods for Heating and Cooling Gases and Apparatus Therefor,” U.S. Patent Number 2,902,337.

[27] Hertzberg, A., and Christiansen, W., 1976, “Method for Continuously Carrying Out a Gas Phase Reaction and Apparatus Therefore,” U.S. Patent Number 3,998,711.

[28] Kielb, R., 2018, “Hydrocarbon Wave Reformer and Method of Use,” US Patent Application 20180215615.

[29] Campbell, M. F., Parise, T., Tulgestke, A. M., Spearrin, R. M., Davidson, D. F., and Hanson, R. K., 2015, “Strategies for Obtaining Long Constant-pressure Test Times in Shock Tubes,” Shock Waves, Vol. 25, pp. 651–665.

[30] Abanades, A., “Low Carbon Production of Hydrogen by Methane Decarbonization,” Chapter 6 in Production of Hydrogen from Renewable Resources, 2015, Springer, pp. 149-177.

[31] Gyarmathy, G., 1983, “How Does the Comprex Pressure-Wave Supercharger Work?,” SAE Paper 830234.

[32] Christiansen, W. H., Hertzberg, A., 1995 “Wave Machinery for Chemical Processing and High-Efficiency Heat Engines,” Proceedings of the 20th International Symposium on Shock Waves, pp. 135-139.

[33] Glass I. I., Patterson, G. N., 1955, “A Theoretical and Experimental Study of Shock-Tube Flows,” Journal of Aeronautical Sciences, Vol. 22, No. 2, pp. 73-100.

[34] Garen, W., and Lensch, G., 1979 “The Double Shock Wave Tube: Experimental Investigation of Shock-Shock Reflections,” Proceeding of the 12th International Symposium on Shock Tubes and Waves, pp. 155-160.

[35] Dai, Y., Zhang, S., Tao, S., and Hu, D., 2017, “Superposition of Two Incident Shocks in R718 Vapor Flows,” International Journal of Heat and Fluid Flow, Vol. 65, pp. 159-165.

[36] Lauer, J., Berchtoldt, M. and Shang, J., 1967, “Continuous Shock Wave Reactor for Chemical Production and Reaction Studies,” Chemical Engineering Science, Vol. 22, pp. 209-215.

[37] Zumdiek, J. F., Vaidyanathan, T. S., Klosterman, E. L., Taussig, R. T., Cassady, P. E., Thayer, W. J., and Christiansen, W. H., 1979 “The Fluid Dynamic Aspects of an Efficient Point Design Energy Exchanger,” Proceeding of the 12th International Symposium on Shock Tubes and Waves, pp. 720-732.

[38] Thayer, W. J., 1985, “The MSNW Energy Exchanger Research Program,” Proceeding ONR/NAVAIR Wave Rotor Research and Technology Workshop, Report NPS-67-85-008, pp. 85-116, Naval Postgraduate School, Monterey, CA.

[39] Tüchler, S., and Copeland, C. D., 2019, “Parametric Numerical Study on the Performance Characteristics of a Micro-Wave Rotor Gas Turbine,” International Gas Turbine Congress, Paper IGTC-2019-200.

[40] Okamoto, K., and Nagashima, T., 2007, “Visualization of Wave Rotor Inner Flow Dynamics,” AIAA Journal of Propulsion and Power, Vol. 23, No. 2, pp. 293-300.

[41] Kurec, K., Piechna, J., and Gumowski, K., 2017, “Investigations on Unsteady Flow Within a Stationary Passage of a Pressure Wave Exchanger by Means of PIV Measurements and CFD Calculations,” Applied Thermal Engineering, Vol. 112, No. 5, pp. 610-620.

[42] Wijeyakulasuriya, S. D., Nalim, M. R., 2012, “Fuel Proximity Effect on Hot-Jet Ignition in a Wave Rotor Constant Volume Combustor,” AIAA Paper 2012-4171.

[43] Li, J., Gong, E., Li, W., Zhang, K, and Yuan, L., 2017, “Investigation on Combustion Properties in Simplified Wave Rotor Constant Volume Combustor,” AIAA Paper 2017-2384.